

Supporting Information

Rachel Wills^{1#}, Jonathan Farhi^{2#}, Patrick Czabala¹, Sophia Shahin¹, Jennifer Spangle², Monika Raj^{1*}

¹Department of Chemistry, Emory University, Atlanta, Georgia 30322, United States

²Department of Radiation Oncology, Winship Cancer Institute of Emory University School of Medicine, Atlanta, GA, United States

Table of Contents	Pages
Supporting Methods	
I. General	2
II. Materials	2
III. Purification	2
IV. Analytical methods	2
V. Cell culture technique	2-3
VI. Experimental Section	3-6
VII. Figure 1: Synthesis of sensor 1a	7-8
VIII. Figure 2: Synthesis of sensor 1b	8-9
IX. Figure 3: Quantum yield of sensor 1a	9-10
X. Figure 4: Quantum yield of sensor 1b	10
XI. Figure 5: Synthesis of sensor products 2a and 3a	11-12
XII. Figure 6: Flow cytometry analysis of cell death by aldehyde sponges	13
XIII. Figure 7: Flow cytometry analysis of cell death by sensor 1a.	13
XIV. Figure 8: Flow cytometry analysis of cell death by aliphatic aldehydes	14
XV. Figure 9: Flow cytometry detection of exogenous aldehydes in live cells	14-15
XVI. Figure 10: Confocal analysis of LNCaP cells treated with aliphatic aldehydes	15
XVII. Figure 11: Confocal analysis of sensor 1a limit of detection	16
XVIII. Figure 12: Confocal microscopy detection of propanal, MGO, and NO levels in live LNCaP cells by sensor 1a	17
XIX. Figure 13: Quantification of Endogenous Aldehydes in the Presence of ALDH-2 Inhibitor and Activator	17
XX. Figure 14: ¹ H and ¹³ C spectra of synthesized compounds	18-24
XXI. Figure 15: HRMS spectra of sensors and products	25-26
XXII. References	26

- I. **General.** All commercial materials (Sigma-Aldrich, TCI, and ThermoFisher) were used without further purification. All solvents were reagent or HPLC (Fisher) grade. Conversions refer to chromatographically pure compounds; percent conversions were obtained by comparison of HPLC peak areas of products and starting materials. Reaction progress was monitored by TLC plates (TLC Silica gel 60 F₂₅₄) and visualized with UV lamps.
- II. **Materials.** 4-amino-3-nitrobenzaldehyde, ethyl 2,4-dimethyl-1H-pyrrole-3-carboxylate, and N-(4-formyl-5-methyl-2-nitrophenyl)acetamide were purchased from Ambeed, Inc. Cell Mask dye and Hoechst 3342 was purchased from ThermoFisher. AV/PI stains (FITC and PacificBlue) were purchased from Biolegend. Cell lines were obtained from the Spanglab Lab at Winship Cancer Institute of Emory University School of Medicine.
- III. **Purification.** All compounds were purified with column chromatography using silica gel, 230-400 mesh, SiliaFlash P60 (Silicycle).
- IV. **Analytical Methods.**

NMR: NMR spectra were recorded on a 400 MHz or 600 MHz Bruker NMR spectrometer. Proton chemical shifts were referenced to residual CDCl₃ at 7.26 ppm and carbon chemical shifts were referenced to CDCl₃ at 77.16 ppm. Spectra were processed using Mnova ver. 12.0.4 and TOPSPIN software. The following abbreviations (or combinations thereof) are used to refer to multiplicities: s = singlet, d = doublet, t = triplet, q = quartet, p = quintet, and m = multiplet. Coupling constants (*J*), are reported in Hertz units (Hz).

HPLC: Chemoselectivity reactions were analyzed using high performance liquid chromatography (HPLC) on an Agilent 1100 series HPLC equipped with a 5 μm particle size, C-18 reversed-phase column. All separations involved a mobile phase of water with 0.1% formic acid (solvent A) and acetonitrile with 0.1% formic acid (solvent B). The HPLC method employed a linear gradient of 30-100% solvent B over 30 minutes at ambient temperature with a flow rate of 1 mL min⁻¹. The eluent was monitored by absorbance at 220 nm and 280 nm.

LC-MS: Reactions were checked on an Agilent 1100 Series HPLC with MSD VL mass spectrometer using positive polarity electrospray ionization (+ESI).

HRMS. High resolution MS data were acquired on a Thermo Exactive Plus using positive-ion electrospray ionization (ESI+). Data were processed with Thermo Scientific Freestyle software ver. 1.8.63.0.

Fluorimeter: Fluorescence spectroscopy was performed with an Agilent Cary Eclipse. Sensor **1a** had an excitation of 485 nm and an emission of 507 nm. Sensor **1b** had an excitation of 485 nm and an emission of 527 nm. Excitation and emission slits were set to five for each experiment.

Microwell Plate Reader: Fluorescence intensity was measured by a Synergy H1 by BioTek. An excitation of 485 nm and an emission of 507 nm was used with Sensor **1a**.

- V. **Cell Culture Technique:** Cells were maintained at 37 °C and 5% CO₂. T47D and

LNCaP cells were cultured in RPMI supplemented with 10% (V/V) fetal bovine serum (FBS), 1% (V/V) penicillin/streptomycin (100 µg/mL), and 1% (V/V) L-glutamate (100 µg/mL). MCF10A cells were cultured in DMEM/F12 supplemented with 3 mL FBS, 1% (V/V) penicillin/streptomycin (100 µg/mL), EGF (20 ng/mL), hydrocortisone (0.5 mg/mL), cholera toxin (100 ng/mL), and insulin (10 µg/mL). Daidzin (DDZ) was purchased from phytolab (89182). Alda-1 was purchased from Sigma Aldrich (SML0462-5MG). The overly adhesive nature of LNCaP cells led to an inability to perform flow cytometry experiments. T47D cells were adopted for these experiments based on favorable morphology.

VI. Experimental Section.

Chemoselectivity studies of sensor 1a with biological compounds. Sensor **1a** (1 mM, 1 equiv.) was incubated in DMSO for 2 h at 37° C with 50 mM (50 equiv.) of the following biological compounds: Formaldehyde, acetaldehyde, propanal, butyraldehyde, valeraldehyde, octanal, benzaldehyde, 4-nitrobenzaldehyde, glutathione (GSH), pyruvate, L-Arg, L-Cys, DL-Hcy, CaCl₂, KNO₃, Na₂SO₃, NaNO₃, H₂O₂, di-tert butyl peroxide (DTBP), SNAP (NO donor), and methylglyoxal. Each reaction was frozen in liquid nitrogen and thawed individually for HPLC analysis and MS verification to determine the percent conversion of sensor **1a** into any modified reactant. All reactions were performed in triplicate.

Rate of benzimidazole formation in solution. The rate of benzimidazole formation was determined upon the reaction of sensor **1a** (10 µM, 1 equiv.) with propanal (1 µM, 0.1 equiv.) in DMSO. The reaction was monitored over 4 h with fluorescence intensity measurements collected every 10 min by fluorimeter. Increases in fluorescence were plotted against time and a one-phase association curve was used to determine the rate constant. The reaction was performed in triplicate.

Rate of benzimidazole formation in cell lysate. The rate of benzimidazole formation in cell lysate was conducted with a fluorimeter. 10 µM of sensor **1a** was added to 50 µg of cell lysate from T47D cells in buffer. The reaction progress was monitored over 1 h with fluorescence intensity measurements collected every 5 min. Maximum fluorescence intensity of each measurement was plotted against time and a one-phase association curve was used to determine the rate constant. The reaction was performed in triplicate. The average of the triplicate was plotted in Fig. 2b for clear visualization.

Rate of benzimidazole formation in live cells. T47D cells were seeded at 10,000 cells/well in a 96-well plate and incubated overnight at 37°C and 5% CO₂. Sensor **1a** (5 µM) was added to wells and immediately analyzed for fluorescence increase over a 1 h period with a microwell plate reader (kinetic run, ex 490, em 507). Twelve trials were performed, and the data was processed using Prism software. The fluorescence intensity of every measurement was plotted against

time and a one-phase association curve was used to determine the rate constant.

Rate of benzimidazole formation in live cells with aldehyde sponges.

Aldehyde sponges, 2,3-diaminophenol (DAP) and 2-amino-4-chlorobenzenethiol (ABT), were used to monitor changes in aliphatic aldehyde concentrations over time. T47D cells were seeded at 10,000 cells/ well in a 96-well plate and incubated overnight. Cells were then treated with DAP (10 μ M or 50 μ M) or ABT (10 μ M or 50 μ M) and cotreated with sensor 1a (5 μ M). Cells were immediately monitored for fluorescence increase over a 1 h period with a microwell plate reader (kinetic run, ex. 490, em. 507). The experiments were performed four times and the data was processed using Prism software. The average of the four runs was plotted in the figure for clear visualization.

Flow cytometry analysis of cell death by aldehyde sponges.

T47D cells were treated with 2,3-diaminophenol (DAP) (10 μ M or 50 μ M) or 2-amino-4-chlorobenzenethiol (ABT) (10 μ M or 50 μ M) for 1 h. After incubation, cells were washed with PBS, detached with trypsin, and stained with Annexin V/PI, according to manufacturer's protocol. Annexin V (AV) conjugated to FITC was used to determine apoptosis and propidium iodide (PI) was used to determine necrosis within the cell population. Cells were analyzed via flow cytometry within 1 h to quantify cell death. FlowJo software was used to analyze data collected on the cytometer. PI and AV controls were used to determine quadrant placement. All the experiments were performed in triplicate.

Flow cytometry analysis of cell death by sensor 1a.

T47D cells were incubated with 5 μ M or 20 μ M of sensor 1a for 24 h with equal amounts of DMSO as control. Cells were then detached with trypsin and stained using Annexin V/PI following manufacturer's protocol. To avoid fluorescent crosstalk, Annexin V (AV) conjugated to PacificBlue was used to determine apoptosis. Propidium Iodide (PI) was used to determine necrosis within the T47D cell population. Cells were analyzed via flow cytometry within 1 h to quantify cell death. FlowJo software was used to analyze the cytometry data. PI and AV controls were used to determine quadrant placement. All the experiments were performed in triplicate.

Flow cytometry analysis of cell death by aliphatic aldehydes.

T47D cells were incubated with of propanal (10 mM or 100 mM) or acetaldehyde (10 mM or 100 mM) for 1 h, detached with trypsin, and stained using Annexin V/PI following manufacturer's protocol. Annexin V (AV) conjugated to FITC was used to determine apoptosis while propidium iodide (PI) was used to determine necrosis within the cell population. Cells were analyzed via flow cytometer within 1 h to quantify cell death. FlowJo software was used to analyze the cytometry data. PI and AV controls were used to determine quadrant placement. All the experiments were performed in triplicate.

Flow cytometry detection of exogenous aldehydes in live cells. MCF10A cells were pretreated with 5 μ M sensor **1a** for 24 h, washed with cold PBS, then treated with propanal or acetaldehyde (10 mM or 100 mM) in supplemented DMEM/F12. After a 1 h aldehyde incubation, cells were washed with PBS, detached with trypsin, and stained with propidium iodide (PI). Cells were analyzed via flow cytometry within 1 h; reacted sensor **1a** was used as a positive control for sensor **1a** staining. PI-negative cells were selected for analysis. Fluorescence intensity was measured via flow cytometry within 1 h and data was analyzed using FlowJo software. All the experiments were performed in triplicate.

Live cell monitoring of exogenous aldehyde level. Live T47D and LNCaP cells were plated on a glass bottomed 8-well plate in supplemented RPMI and incubated for 24 h. Cells were then incubated with 10 μ M concentrations of sensor **1a**. After 24 h, the cells were washed with PBS and incubated with propanal or acetaldehyde (10 mM) for 1 h. Prior to imaging, cells were stained with 1 μ g/mL Hoechst for 5 min. Cells were then placed in fresh RPMI media. Cells were imaged on Leica SP8 confocal microscope and images were processed and analyzed using ImageJ software. All the experiments were performed in triplicate.

Sensor 1a limit of detection of exogenous aldehyde in live cells. Live LNCaP cells were plated on a glass bottomed 8-well plate in supplemented RPMI media and incubated for 24 h at 37°C and 5% CO₂. Cells were then treated with 10 μ M of sensor **1a** and incubated for an additional 24 h. Cells were washed with PBS and incubated with increasing levels of propanal (2 μ M, 4 μ M, 6 μ M, 8 μ M, 10 μ M) for 1 h. Prior to imaging, cells were stained with Cell Mask and incubated for 10 min. Cells were subsequently washed 3 times in cold PBS (5 min) and stained with 1 μ g/mL Hoechst for 5 min. Cells were then placed in fresh RPMI media and imaged on Leica SP8 confocal microscope. The images were processed and analyzed using ImageJ to determine pixel intensity per cell. All the experiments were performed in triplicate.

Live cell detection of propanal, MGO, and NO levels. Live LNCaP cells were plated on a glass bottomed 8-well plate in supplemented RPMI and incubated for 24 h. Cells were treated with 10 μ M concentrations of sensor **1a**. After 24 h, the cells were washed with PBS and incubated with propanal (20 μ M), MGO (5 μ M), or SNAP (0.5 μ M) at their physiological concentrations inside cells for 1 h. Prior to imaging, cells were stained with 1 μ g/mL Hoechst for 5 min. Cells were then placed in fresh RPMI media. Cells were imaged on Leica SP8 confocal microscope, and the images were processed and analyzed using ImageJ software to determine pixel intensity per cell.

Live cell monitoring of acetaldehyde levels through the addition of ethanol and ALDH2 inhibitor. Live LNCaP cells were plated on glass bottomed 35 mm dishes in supplemented RPMI and incubated for 24 h. Cells were then incubated with 5 μ M concentrations of sensor **1a** with or without ALDH2 inhibitor, DDZ (5

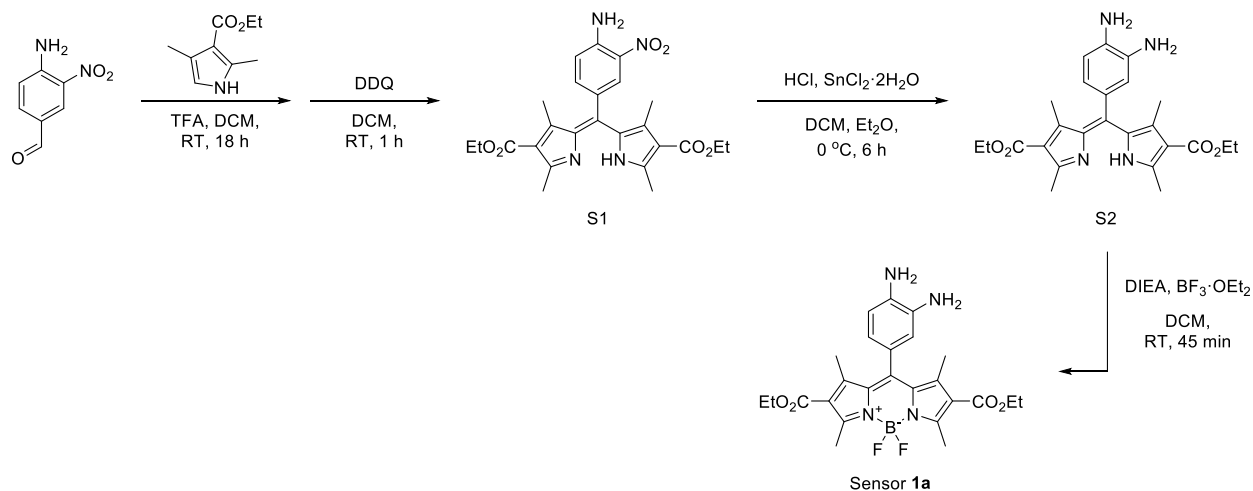
μM). After 24 h, the cells were washed once with PBS, then incubated with 10 mM ethanol for 1h. 10 min prior to imaging, cells were placed in DMEM/F12 media without phenol red containing 1 $\mu\text{g}/\text{mL}$ Hoechst. Cells were imaged on Leica SP8 confocal microscope and images were processed and analyzed using ImageJ and Python software.

Cellular kinetics in the presence of ALDH2 activator and inhibitor. T47D cells were seeded at 10,000 cells/well on a 96-well plate and incubated overnight at 37°C and 5% CO₂. After treatment with or without ALDH2 inhibitor (DDZ, 5 or 20 μM) or ALDH2 activator (Alda-1, 50 or 100 μM), sensor **1a** (5 μM) was added to wells and the cells were immediately analyzed by microwell plate reader to measure fluorescence over a 1 h period (kinetic run, ex. 490, em. 507). Twelve trials were performed, and the data was processed using Prism software.

Live cell monitoring of endogenous aldehyde levels in the presence of ALDH2 activator and inhibitor. Live LNCaP cells were plated on glass bottomed 8-well plates in supplemented RPMI media and incubated for 24 h. Cells were then treated with 10 μM of sensor **1a** with or without DDZ (20 μM) or Alda-1 (20 μM). After 1 h, cells were stained with Cell Mask and incubated for 10 min. Cells were subsequently washed 3 times with PBS (5 min) and stained with 1 $\mu\text{g}/\text{mL}$ Hoechst for 5 min. Cells were then placed in fresh supplemented RPMI media and imaged on Leica SP8 confocal microscope. The images were processed and analyzed using ImageJ software to determine pixel intensity per cell. Data was normalized to sensor 1a only wells to show increases and decreases in intensity signal from DDz and Alda-1, respectively.

Live cell monitoring of fluorescence intensity upon addition of sensor 1a. Live LNCaP cells were plated on glass bottomed 8-well plates in supplemented RPMI media and incubated for 24 h. Cells were then stained with Cell Mask and incubated for 10 min. Cells were then washed 3 times in PBS (5 min) and stained with 1 $\mu\text{g}/\text{mL}$ Hoechst for 5 min. Cells were washed with PBS and placed in fresh supplemented RPMI. Cells were then imaged on Nikon Crestoptics X-Light V2 L-FOV. After initial imaging, 10 μM of sensor **1a** was added directly to cells. Images were taken every 1 min for 60 min following sensor **1a** addition.

VII. Supplementary Figure 1: Synthesis of Sensor 1a.¹



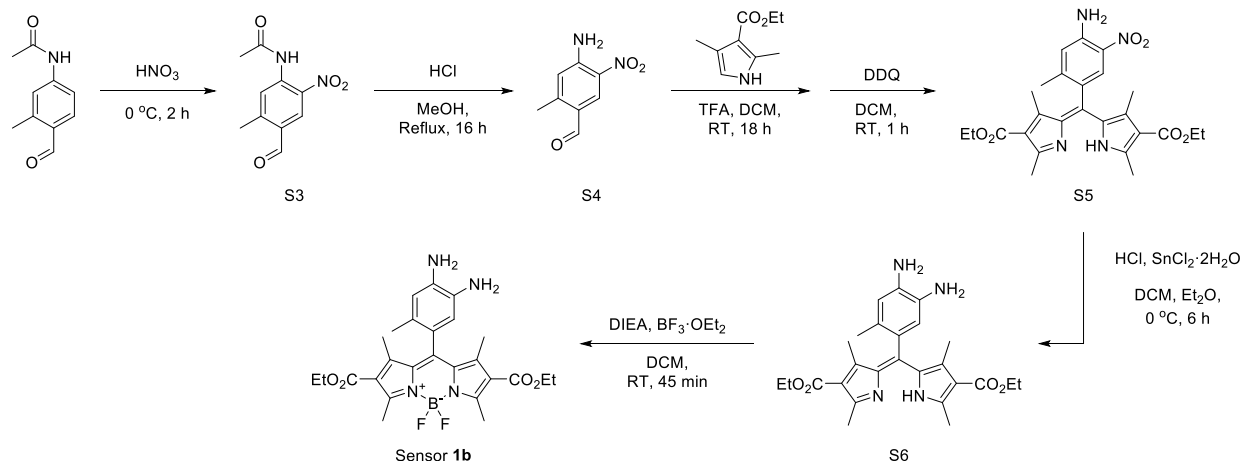
Ethyl (Z)-5-((4-amino-3-nitrophenyl)(4-(ethoxycarbonyl)-3,5-dimethyl-2H-pyrrol-2-ylidene)methyl)-2,4-dimethyl-1H-pyrrole-3-carboxylate (S1): 4-amino-3-nitrobenzaldehyde (250 mg, 1.5 mmol) and ethyl 2,4-dimethyl-1H-pyrrole-3-carboxylate (503 mg, 3.0 mmol) were dissolved in anhydrous DCM (60 mL) under nitrogen atmosphere. One drop of TFA was added and the reaction was monitored by TLC for the consumption of the 4-amino-3-nitrobenzaldehyde. DDQ (341 mg, 1.5 mmol), pre-dissolved in DCM, was added to the reaction and monitored over 1 h by TLC. The reaction was washed with water (20 mL) and extracted with DCM (3 x 10 mL) before drying with MgSO₄ and evaporating excess solvent. S1 was purified by column chromatography (9:1 EtOAc:Hexane) with the addition of TEA in the mobile phase. Bright orange solid was obtained (304 mg, 42% yield). ¹H NMR (400 MHz, CDCl₃) δ 6.84 (d, *J* = 8.3 Hz, 1H), 6.60 – 6.55 (m, 2H), 4.30 (q, *J* = 7.1 Hz, 1H), 2.84 (s, 1H), 1.84 (s, 1H), 1.35 (t, *J* = 7.1 Hz, 1H). ¹³C NMR (151 MHz, CDCl₃) δ 164.46, 158.90, 147.87, 147.00, 136.20, 135.79, 131.90, 125.54, 122.19, 119.56, 117.20, 115.64, 60.15, 53.42, 14.93, 14.30, 13.96.

ethyl (Z)-5-((3,4-diaminophenyl)(4-(ethoxycarbonyl)-3,5-dimethyl-2H-pyrrol-2-ylidene)methyl)-2,4-dimethyl-1H-pyrrole-3-carboxylate (S2): S1 (190 mg, 0.32 mmol) was dissolved in DCM (20 mL) and 2 M HCl in diethyl ether (20 mL) and cooled on ice. Tin chloride dihydrate (1.1 g, 4.9 mmol) was added portion-wise and stirred for 6 h. The reaction was concentrated and diluted with 2 M NaOH, followed by an extraction with DCM. The organic layer was dried with MgSO₄ and concentrated before immediate use in the next synthetic step.

diethyl 10-(3,4-diaminophenyl)-5,5-difluoro-1,3,7,9-tetramethyl-5H-4λ⁴,5λ⁴-dipyrrolo[1,2-c:2',1'-f][1,3,2]diazaborinine-2,8-dicarboxylate (1a): S2 was reconstituted in anhydrous DCM (20 mL) under nitrogen atmosphere. Diisopropylethylamine (325 mg, 2.5 mmol) was added and stirred at room temperature for 10 min. BF₃(OEt)₂ (477 mg, 3.36 mmol) was added dropwise and stirred for 45 min before the reaction was cooled in an ice bath and quenched with 2 M NaOH (5 mL) and water (20 mL). The aqueous layer was extracted with DCM (3 x 20 mL), dried with MgSO₄, and concentrated followed by purification using column chromatography (3:2 EtOAc:Hexane). Sensor 1a was generated as a shiny black purple solid (25 mg, 13% yield over 2 steps). ¹H NMR (600 MHz, CDCl₃) δ 6.82 (d, *J* = 8.4 Hz, 1H), 6.57 – 6.53

(m, 2H), 4.27 (q, $J = 7.1$ Hz, 4H), 2.81 (s, 6H), 1.81 (s, 6H), 1.32 (t, $J = 7.1$ Hz, 6H). ^{13}C NMR (101 MHz, CDCl_3) δ 165.21, 155.71, 145.37, 145.08, 140.58, 137.13, 136.71, 132.25, 127.48, 125.62, 121.11, 119.55, 77.36, 77.04, 76.72, 59.81, 17.57, 14.60, 14.38.

VIII. Supplementary Figure 2: Synthesis of Sensor 1b.¹



N-(4-formyl-5-methyl-2-nitrophenyl)acetamide (S3): N-(4-Formyl-3-methylphenyl)acetamide (1032 mg, 5.8 mmol) was aliquoted into reaction vials at ~250 mg and cooled to 0 °C with ice. Fuming nitric acid (900 μL) was added to each reaction and stirred for 2 h. The reaction mixtures were then poured over ice to induce precipitation and combined. The resulting solid was filtered out and dissolved in DCM before washing with brine and drying with MgSO_4 . S3 was purified with column chromatography (1:5 EtOAc:Hexane). Yellow solid was obtained (280 mg, 21.6% yield). ^1H NMR (400 MHz, CDCl_3) δ 10.62 (s, 1H), 10.14 (s, 1H), 8.77 (s, 1H), 8.66 (s, 1H), 2.74 (s, 3H), 2.33 (s, 3H). ^{13}C NMR (101 MHz, CDCl_3) δ 189.41, 169.28, 149.46, 138.33, 133.94, 130.25, 128.89, 123.91, 25.87, 20.32.

4-amino-2-methyl-5-nitrobenzaldehyde (S4): S3 (280 mg, 1.26 mmol) was dissolved in 30 mL of 2M HCl:MeOH (1:4) solution and refluxed for 16 h under nitrogen atmosphere. The solution was concentrated and then diluted with water (10 mL) and 2M NaOH (10 mL). The product was extracted with DCM (3 x 10 mL), dried with MgSO_4 , and concentrated. S4 was purified with column chromatography (3:2 EtOAc:Hexane) to yield a yellow solid (202 mg, 89% yield). ^1H NMR (600 MHz, CDCl_3) δ 9.92 (s, 1H), 8.56 (s, 1H), 6.63 (s, 1H), 2.62 (s, 3H). ^{13}C NMR (101 MHz, CDCl_3) δ 189.81, 148.09, 147.36, 134.32, 125.00, 120.60, 20.55.

Ethyl (Z)-5-((4-amino-2-methyl-5-nitrophenyl)(4-(ethoxycarbonyl)-3,5-dimethyl-2H-pyrrol-2-ylidene)methyl)-2,4-dimethyl-1H-pyrrole-3-carboxylate (S5): S4 (195 mg, 1.08 mmol) and ethyl 2,4-dimethyl-1H-pyrrole-3-carboxylate (362 mg, 2.16 mmol) were dissolved in anhydrous DCM (60 mL) under nitrogen atmosphere. One drop of TFA was added and the reaction was monitored by TLC for the consumption of S4. DDQ (245 mg, 1.08 mmol), pre-dissolved in DCM, was added to the reaction and monitored over 1 h by TLC. The reaction was washed with water (20 mL) and extracted with DCM (3 x 10 mL), dried with MgSO_4 , and concentrated. S5 was purified by column chromatography (9:1 EtOAc:Hexane) with the addition of TEA in the mobile phase. Bright orange solid was obtained (379 mg, 36.4% yield).

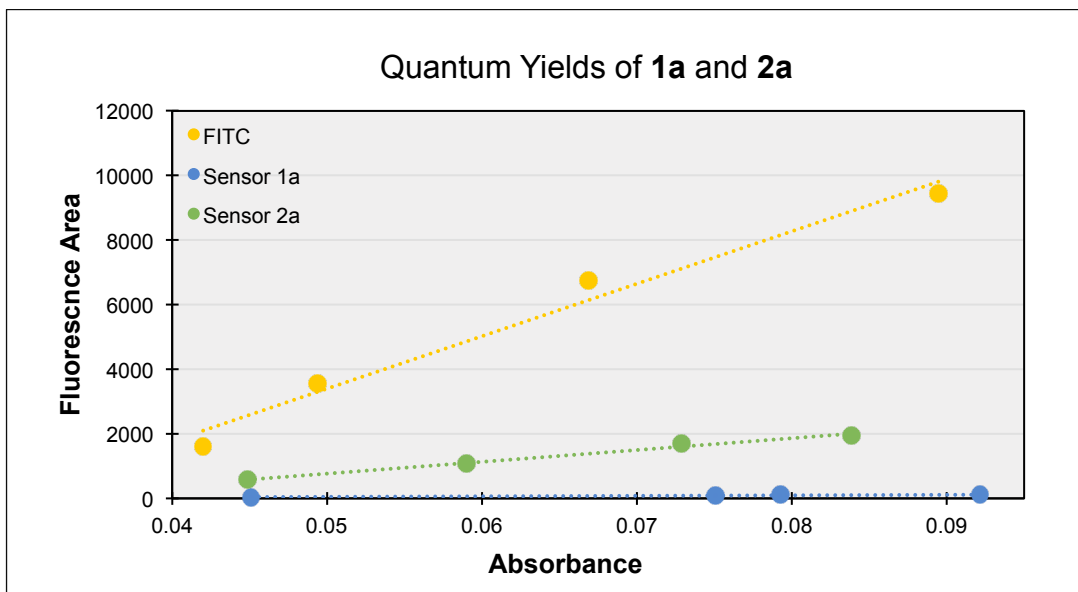
Ethyl (Z)-5-((4,5-diamino-2-methylphenyl)(4-(ethoxycarbonyl)-3,5-dimethyl-2H-pyrrol-2-ylidene)methyl)-2,4-dimethyl-1H-pyrrole-3-carboxylate (S6): S5 (380 mg, 0.77 mmol) was dissolved in DCM (25 mL) and 2 M HCl in diethyl ether (25 mL), then cooled to 0 °C. Tin chloride dihydrate (2.6 g, 11.5 mmol) was added portion-wise and stirred for 6 h. The reaction was concentrated and diluted with 2 M NaOH, followed by an extraction with DCM. The organic layer was dried with MgSO₄ and concentrated before immediate use in the next synthetic step.

Diethyl 10-(4,5-diamino-2-methylphenyl)-5,5-difluoro-1,3,7,9-tetramethyl-5H-4λ⁴,5λ⁴-dipyrrolo[1,2-c:2',1'-f][1,3,2]diazaborinine-2,8-dicarboxylate (1b): S6 was reconstituted in anhydrous DCM (25 mL) under nitrogen atmosphere. Diisopropylethylamine (1.3 g, 10 mmol) was added and stirred at room temperature for 10 min. BF₃(OEt)₂ (1.9 g, 13.4 mmol) was added dropwise and stirred for 45 min before the reaction was cooled in an ice bath and quenched with 2 M NaOH (5 mL) and water (20 mL). The aqueous layer was extracted with DCM (3 x 20 mL), dried with MgSO₄, and concentrated followed by purification with column chromatography (3:2 EtOAc:Hexane). Recrystallization with chloroform and hexane was performed to produce **1b** as shiny black purple powder. (107 mg, 27% yield over 2 steps). ¹H NMR (600 MHz, CDCl₃) δ 6.63 (s, 1H), 6.42 (s, 1H), 4.26 (q, *J* = 7.1 Hz, 4H), 2.80 (s, 6H), 1.96 (s, 3H), 1.79 (s, 6H), 1.31 (t, *J* = 7.1 Hz, 6H). ¹³C NMR (101 MHz, CDCl₃) δ 164.48, 158.89, 147.62, 146.85, 136.57, 133.79, 131.60, 126.34, 124.58, 122.08, 118.55, 115.49, 60.19, 18.39, 14.96, 14.30, 13.07.

IX. Supplementary Figure 3: Quantum yield determination of sensor 1a. Quantum yield was calculated using the area under the curve of fluorescence versus absorption. Fluorescence area was measured with a Cary Eclipse fluorimeter at the following concentrations: 100 nM, 250 nM, 500 nM, and 750 nM. Absorption was measured with a Cary 3500 UV-Vis utilizing the same sample concentrations described above. All measurements were run in triplicate. Quantum yields of sensor **1a** and the corresponding propanal product (sensor **2a**) were determined using FITC as a reference compound. The following equation was used to calculate quantum yield:

$$Q = Q_r \times \frac{m}{m_r} \times \left(\frac{n}{n_r}\right)^2$$

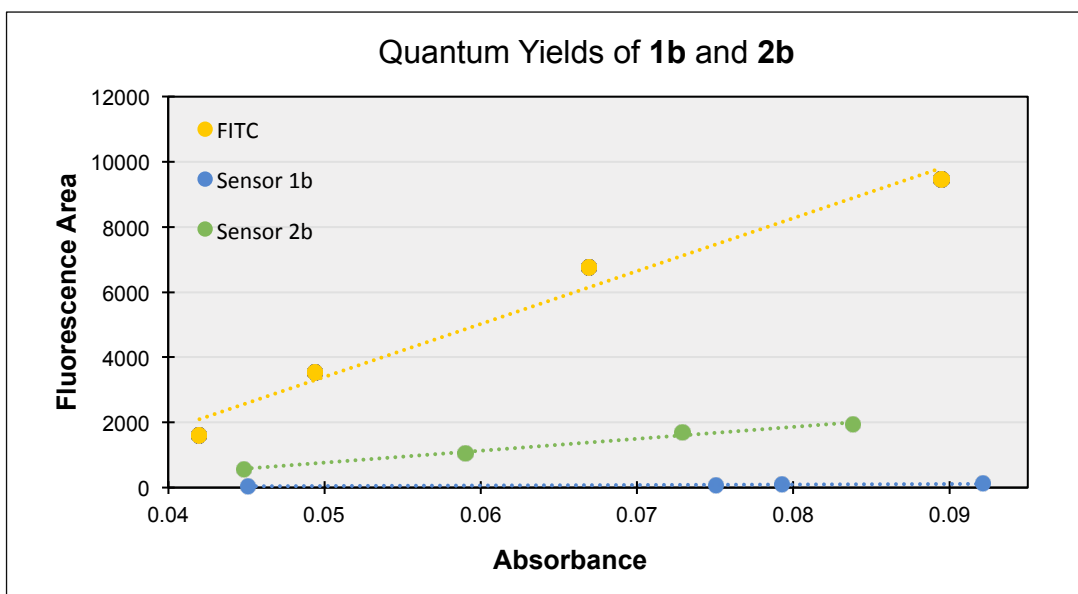
Q is the quantum yield; *m* is the slope of the line described above; *n* is the refractive index of the solvent. Subscript *r* denotes the appropriate values for the reference (FITC).



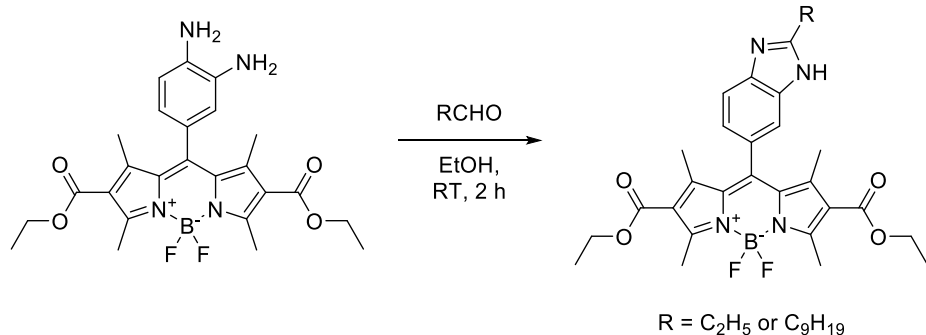
X. Supplementary Figure 4: Quantum yield determination of sensor 1b. Fluorescence area of sensor **1b** and the corresponding propanal product **2b** was measured with a Cary Eclipse fluorimeter at the following concentrations: 100 nM, 250 nM, 500 nM, and 750 nM. Absorption was measured with Cary 3500 UV-Vis utilizing the same sample concentrations described above. All measurements were run in triplicate. Quantum yields of sensor **1b** and propanal product (sensor **2b**) were determined using FITC as a reference compound. The following equation was used to calculate quantum yield:

$$Q = Q_r \times \frac{m}{m_r} \times \left(\frac{n}{n_r}\right)^2$$

Q is the quantum yield; m is the slope of the line described above; n is the refractive index of the solvent. Subscript r denotes the appropriate values for the reference (FITC).



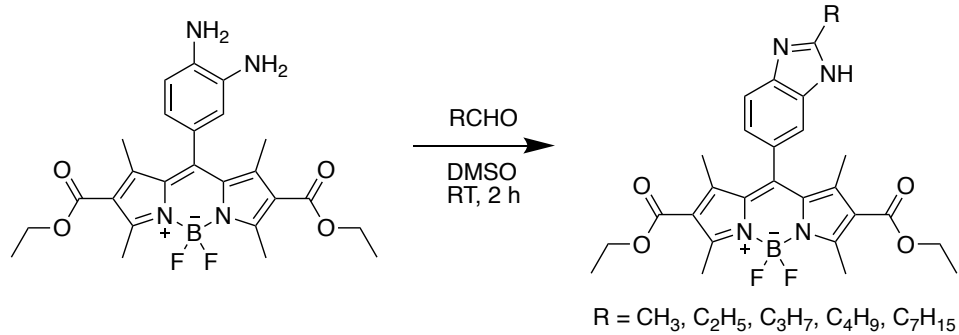
XI. Supplementary Figure 5: Synthesis of sensor products 2a and 3a.



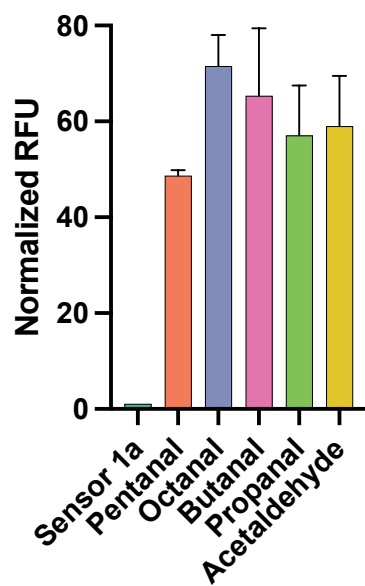
Diethyl 10-(2-ethyl-1H-benzo[d]imidazol-6-yl)-5,5-difluoro-1,3,7,9-tetramethyl-5H-4 λ^4 ,5 λ^4 -dipyrrolo[1,2-c:2',1'-f][1,3,2]diazaborinine-2,8-dicarboxylate (2a). 50 mg of sensor **1a** was reacted with propanal (20 equiv.) in 1.5 mL of ethanol for 2 h to give product **2a**. Silica was added directly to the reaction mixture to make a slurry for purification. Product **2a** was purified with column chromatography (3:2 EtOAC:Hexane) to produce an orange solid (29.8 mg, 52% yield). ¹H NMR (400 MHz, CDCl₃) δ 7.70 (d, *J* = 8.2 Hz, 1H), 7.44 (s, 1H), 7.09 (d, *J* = 8.2 Hz, 1H), 4.29 (q, *J* = 7.1 Hz, 4H), 3.03 (q, *J* = 7.6 Hz, 2H), 2.86 (s, 6H), 1.59 (s, 6H), 1.51 (t, *J* = 7.6 Hz, 3H), 1.33 (t, *J* = 7.1 Hz, 6H). ¹³C NMR (101 MHz, CDCl₃) δ 164.44, 159.30, 157.73, 147.91, 146.65, 131.96, 128.03, 122.42, 121.80, 77.35, 77.03, 76.71, 60.29, 31.94, 29.71, 22.64, 15.03, 14.27, 14.13, 13.81, 11.82.

Diethyl 5,5-difluoro-1,3,7,9-tetramethyl-10-(2-nonyl-1H-benzo[d]imidazol-6-yl)-5H-4 λ^4 ,5 λ^4 -dipyrrolo[1,2-c:2',1'-f][1,3,2]diazaborinine-2,8-dicarboxylate (3a). 50 mg of sensor **1a** was reacted with decanal (20 equiv.) in 1.5 mL of ethanol for 2 h to give product **3a**. Silica was added directly to the reaction mixture to make a slurry for purification. Product **3a** was purified with column chromatography (3:7 EtOAC:Hexane) to produce an orange solid (31.7 mg, 50% yield). ¹H NMR (400 MHz, CDCl₃) δ 7.93 – 7.37 (m, 2H), 7.07 (d, *J* = 8.2 Hz, 1H), 4.28 (q, *J* = 7.1 Hz, 4H), 2.96 (t, *J* = 8.0 Hz, 2H), 2.86 (s, 6H), 1.92 (p, *J* = 7.7 Hz, 2H), 1.59 (s, 6H), 1.45 (p, *J* = 7.7 Hz, 2H), 1.33 (t, *J* = 7.1 Hz, 6H), 1.27 (s, 10H), 0.89 (t, *J* = 6.6 Hz, 3H). ¹³C NMR (101 MHz, CDCl₃) δ 164.47, 159.27, 157.02, 147.94, 146.81, 131.98, 122.39, 121.60, 77.36, 77.04, 76.72, 60.29, 31.94, 31.86, 29.71, 29.52, 29.50, 29.42, 29.32, 29.27, 27.94, 22.67, 15.03, 14.27, 14.11, 13.81.

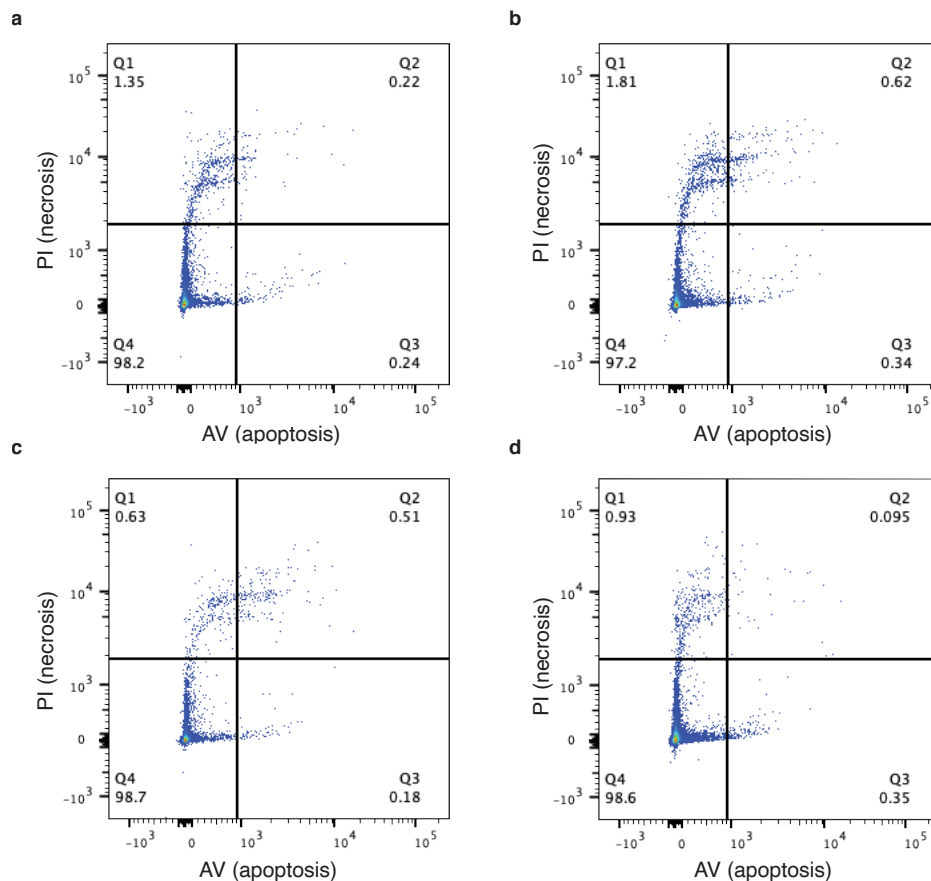
Fluorescence Characterization of Aldehydes with Sensor 1a. Sensor **1a** (10 μ M) was incubated with 50 eq. of various aldehydes for two hours. Reactions were then run in a Cary Eclipse spectrofluorometer to determine fluorescence intensity. Reactions were run in triplicate.



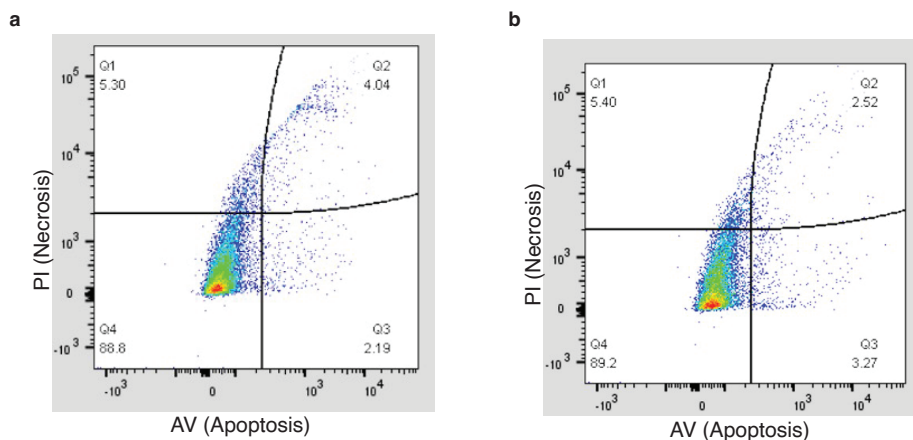
Fluorescence Intensity of Aldehyde Products



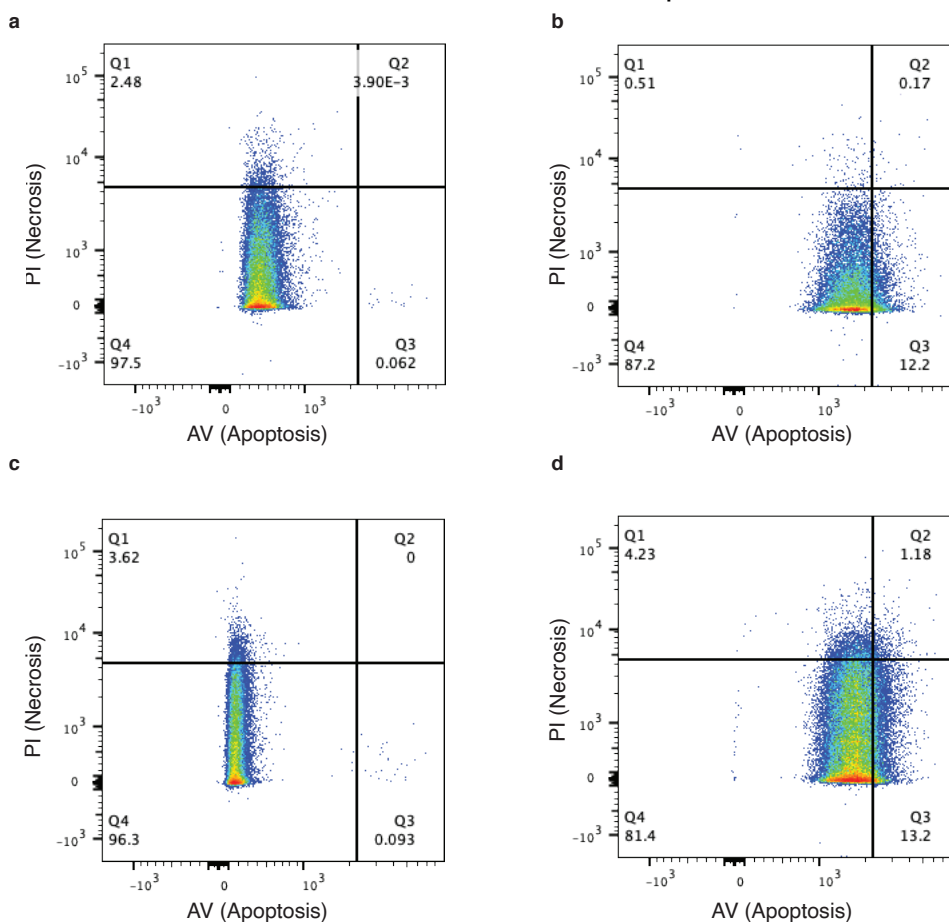
XII. Supplementary Figure 6: Flow cytometry analysis of cell death by aldehyde sponges. No additional cell death was observed compared to control for T47D cells treated for 1h with **a**, 2,3-diaminophenol (10 μ M) **b**, 2,3-diaminophenol (50 μ M) and **c**, 2-amino-4-chlorobenzenethiol (10 μ M) **d**, 2-amino-4-chlorobenzenethiol (50 μ M).



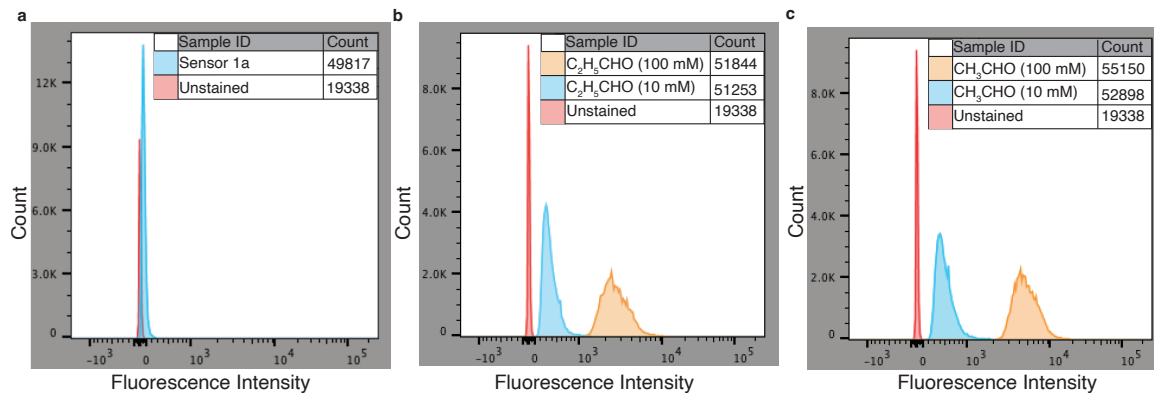
XIII. Supplementary Figure 7: Flow cytometry analysis of cell death by sensor 1a. **a**, Cell death of T47D cells treated with sensor 1a (5 μ M) for 24 h. **b**, Cell death of T47D cells treated with sensor 1a (20 μ M) for 24 h. All the experiments showed no increase in cell death as compared to control.



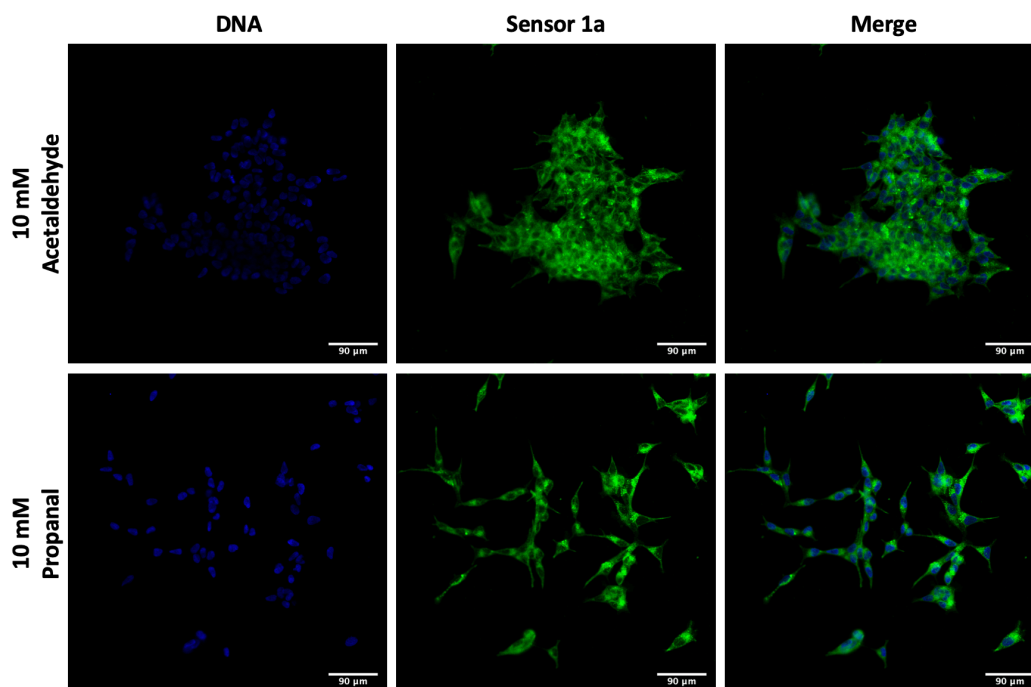
XIV. Supplementary Figure 8: Flow cytometry analysis of cell death by aliphatic aldehydes. **a**, Cell death of T47D cells treated with propanal (10 mM) for 1h. **b**, Flow cytometry data for T47D cells treated with propanal (100 mM) for 1h. **c**, Flow cytometry data for T47D cells treated with acetaldehyde (10 mM) for 1h. **d**, Flow cytometry data for T47D cells treated with acetaldehyde (100 mM) for 1h. No increase in cell death was observed as compared to control for all conditions.



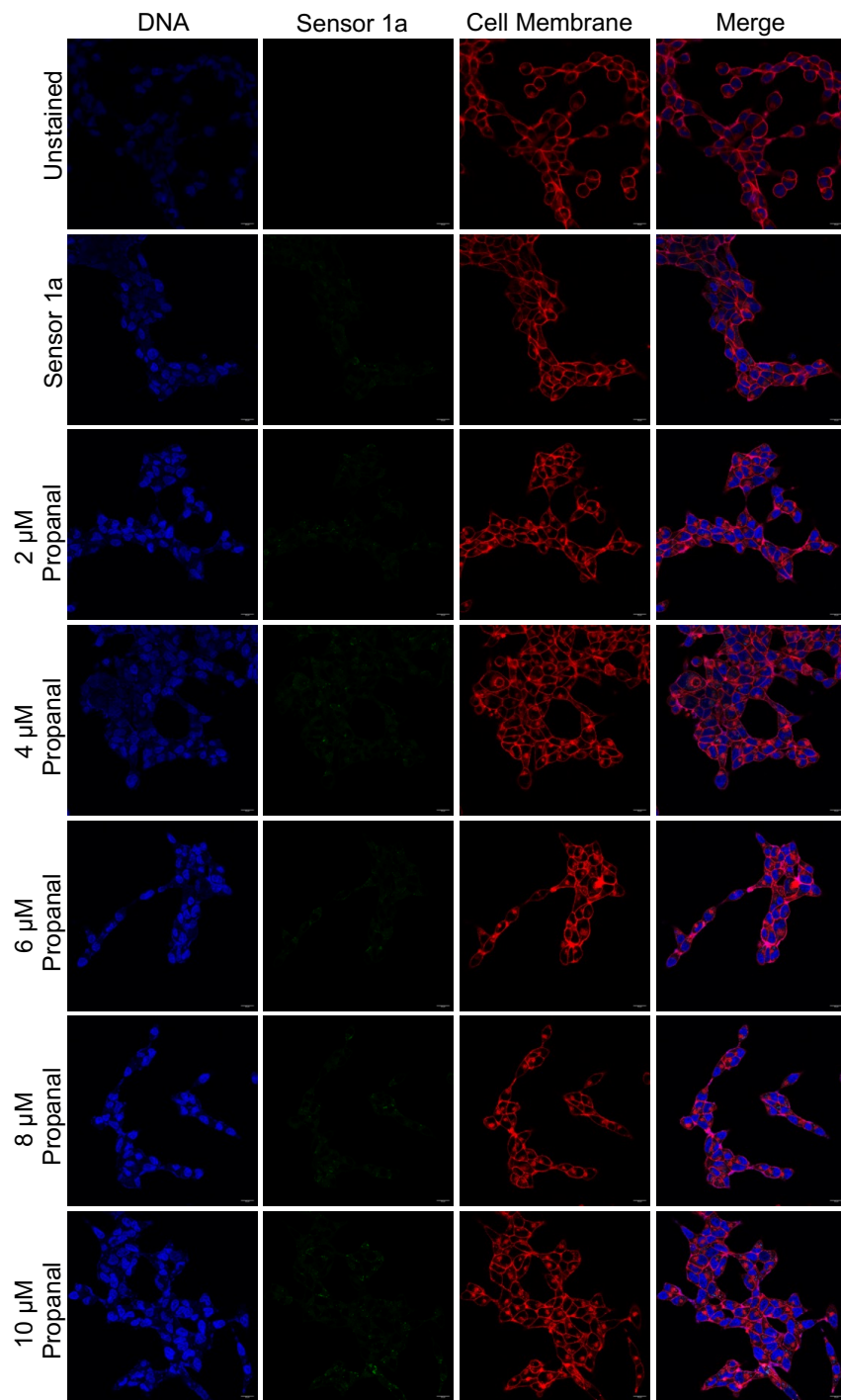
XV. Supplementary Figure 9: Flow cytometry detection of exogenous aldehydes in live cells. **a**, MCF10A cells treated with sensor 1a (5 μ M) for 24 h showed a slight increase in fluorescence intensity as compared to unstained. **b**, Sensor 1a (5 μ M) treated MCF10A cells with propanal (10 mM or 100 mM) for 1 h showed a high increase in fluorescence intensity as compared to unstained and sensor 1a. **c**, Sensor 1a (5 μ M) pretreated MCF10A cells with acetaldehyde (10 mM or 100 mM) for 1 h showed the highest increases in fluorescence intensity as compared to unstained and sensor 1a.



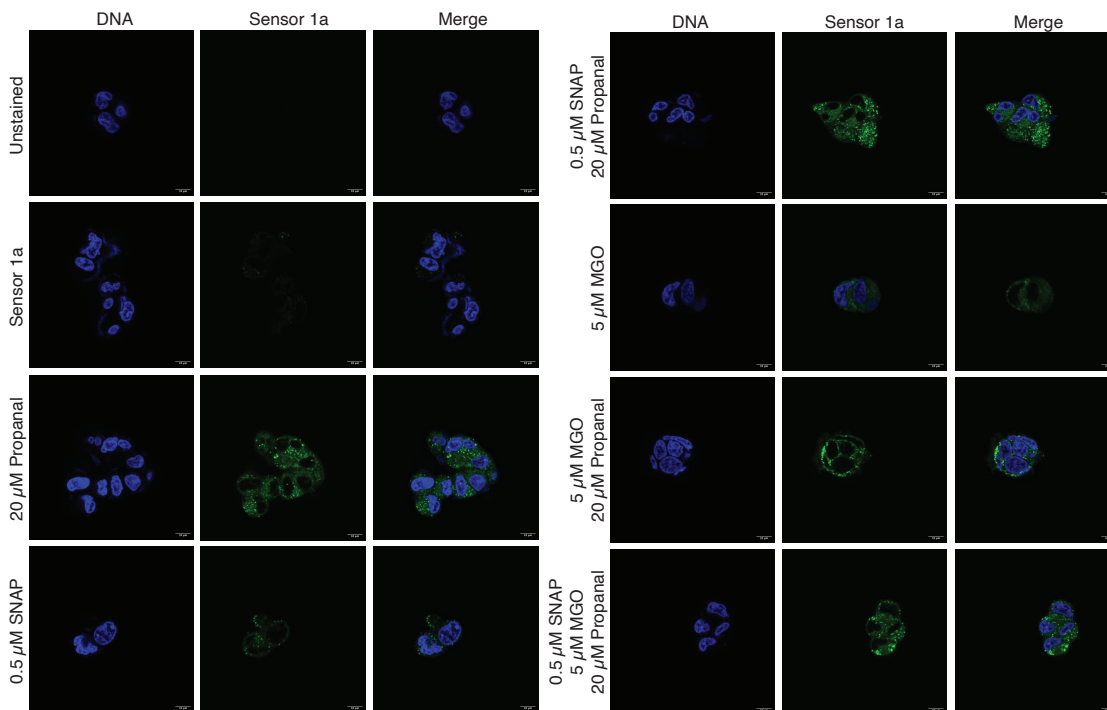
XVI. Supplementary Figure 10: Confocal analysis of LNCaP cells treated with aliphatic aldehydes. The addition of pathological concentrations (10 mM) of acetaldehyde (top) or propanal (bottom) to LNCaP cells pretreated with sensor 1a (10 μ M) showed significant increases in fluorescence intensity as compared to cells treated with sensor 1a only.



XVII. Supplementary Figure 11: Confocal analysis of sensor 1a limit of detection. LNCaP cells pretreated with sensor 1a (10 μ M) showed expected increases in fluorescence intensity in correlation with increasing concentrations of propanal (2 μ M, 4 μ M, 6 μ M, 8 μ M, and 10 μ M). Images were taken after 1h incubation with propanal. All the experiments showed similar trends.

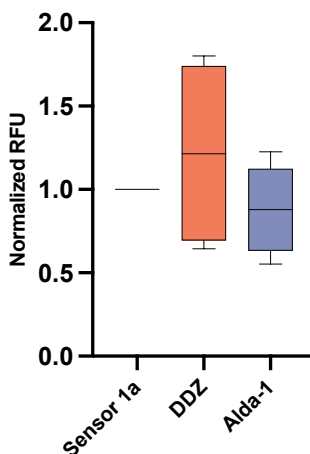


XVIII. Supplementary Figure 12: Confocal microscopy detection of propanal, MGO, and NO levels in live LNCaP cells by sensor 1a. Physiologically relevant levels of propanal, MGO, and SNAP (NO Donor) were added to LNCaP cells pretreated with sensors 1a (10 μ M) and imaged with confocal microscopy. Image analysis shows lower fluorescence intensity upon reaction of sensor 1a with MGO and NO in comparison to an aliphatic aldehyde at their respective physiological concentrations.

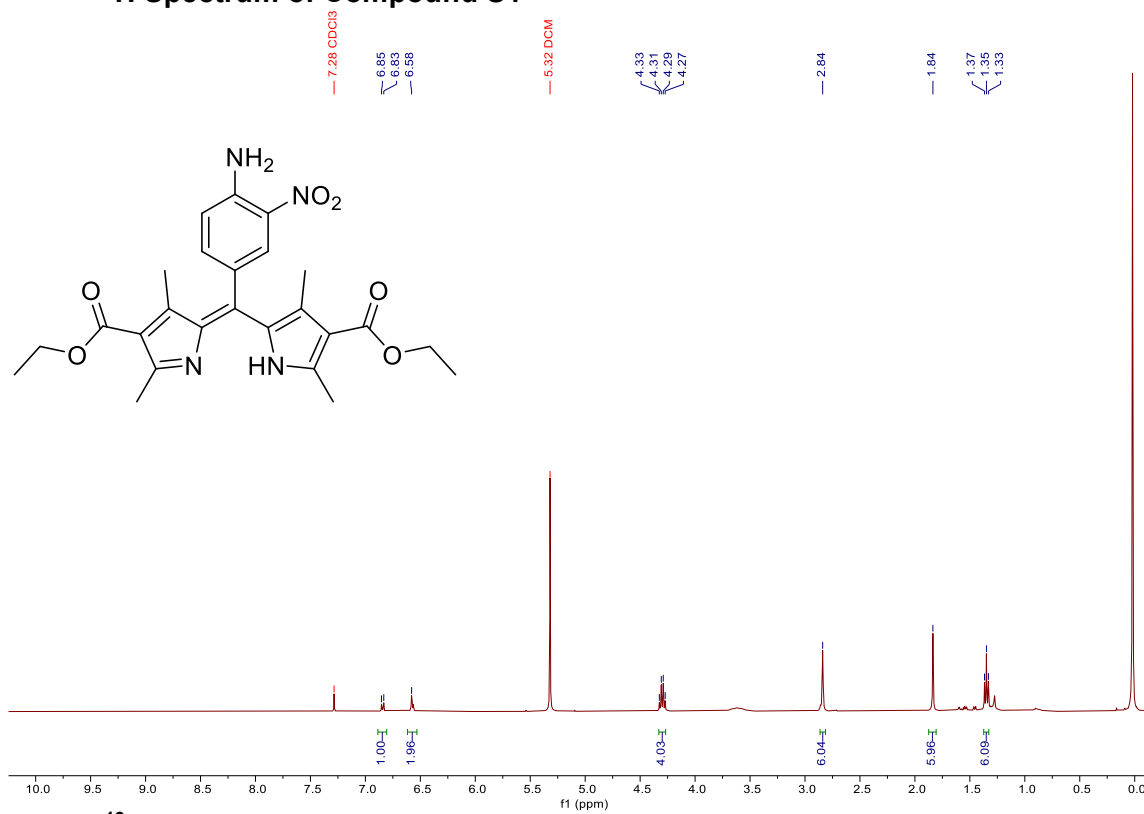


XIX. Supplementary Figure 13: Live cell monitoring of endogenous aldehyde levels in the presence of ALDH2 activator and inhibitor. Cells were treated with 10 μ M of sensor 1a with or without DDZ (20 μ M) or Alda-1 (20 μ M). Average pixel intensity per area shows that the addition of DDZ increases pixel intensity, while the addition of Alda-1 decreases signal. These results are as expected in relation to the concentration of available aldehydes in the cells.

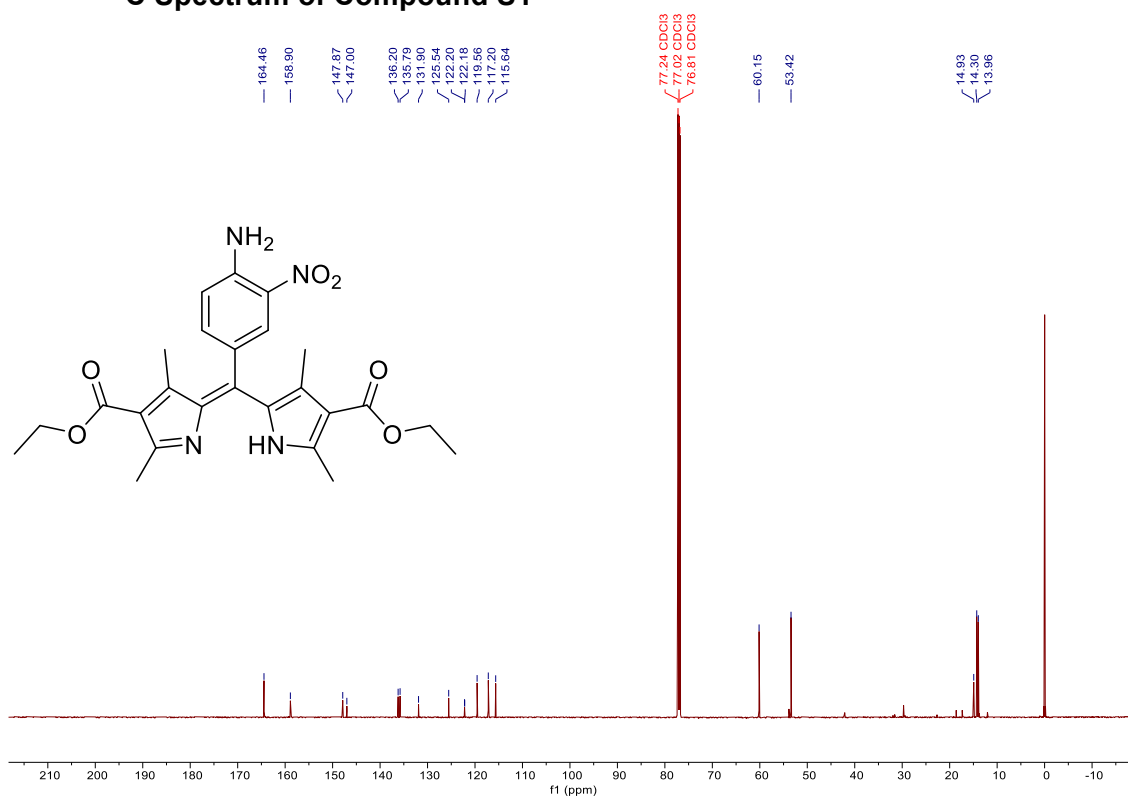
Quantification of Figure 6c



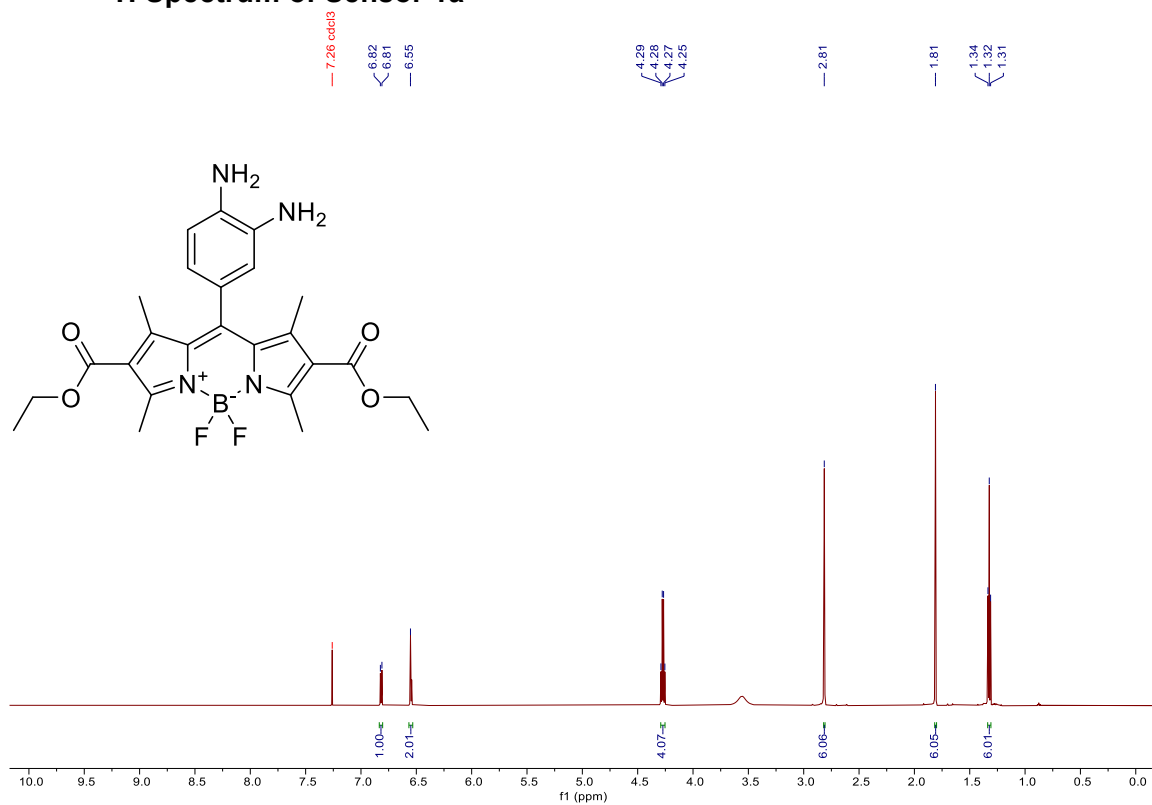
XX. Supplementary Figure 14: NMR Spectra of Synthesized Compounds.
¹H Spectrum of Compound S1



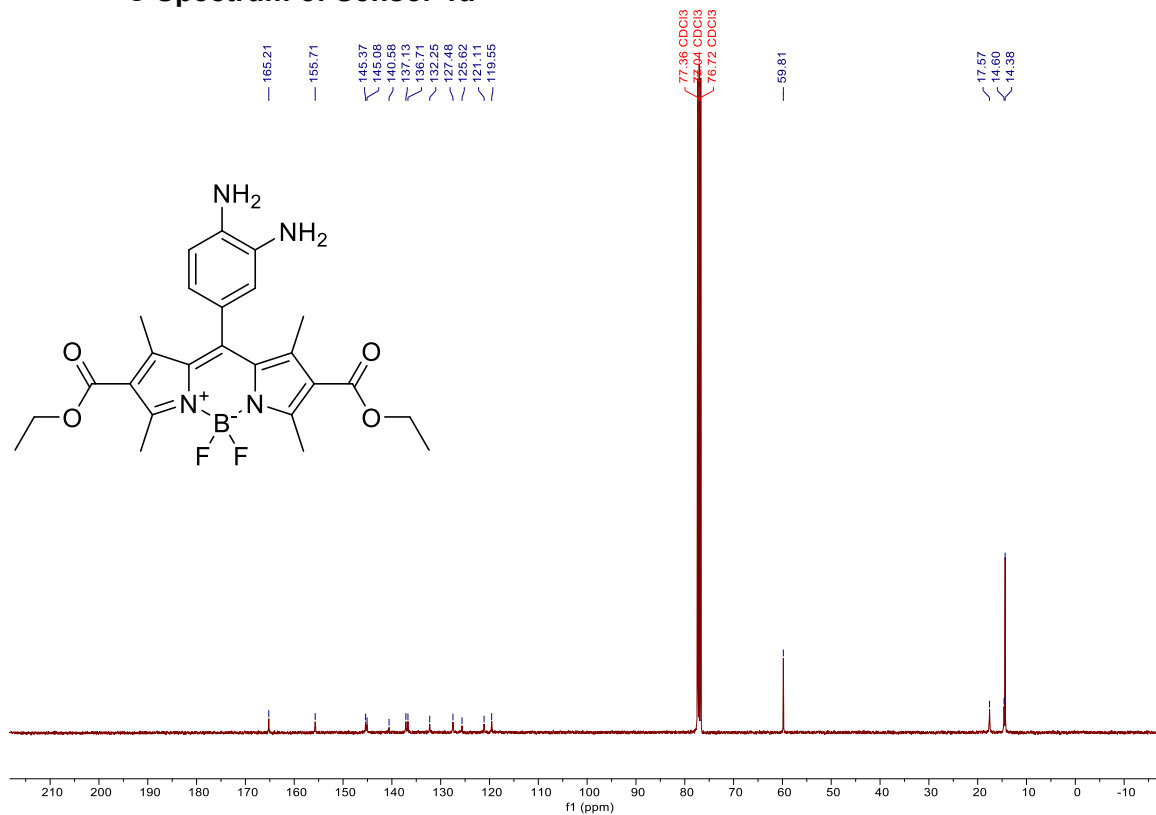
¹³C Spectrum of Compound S1



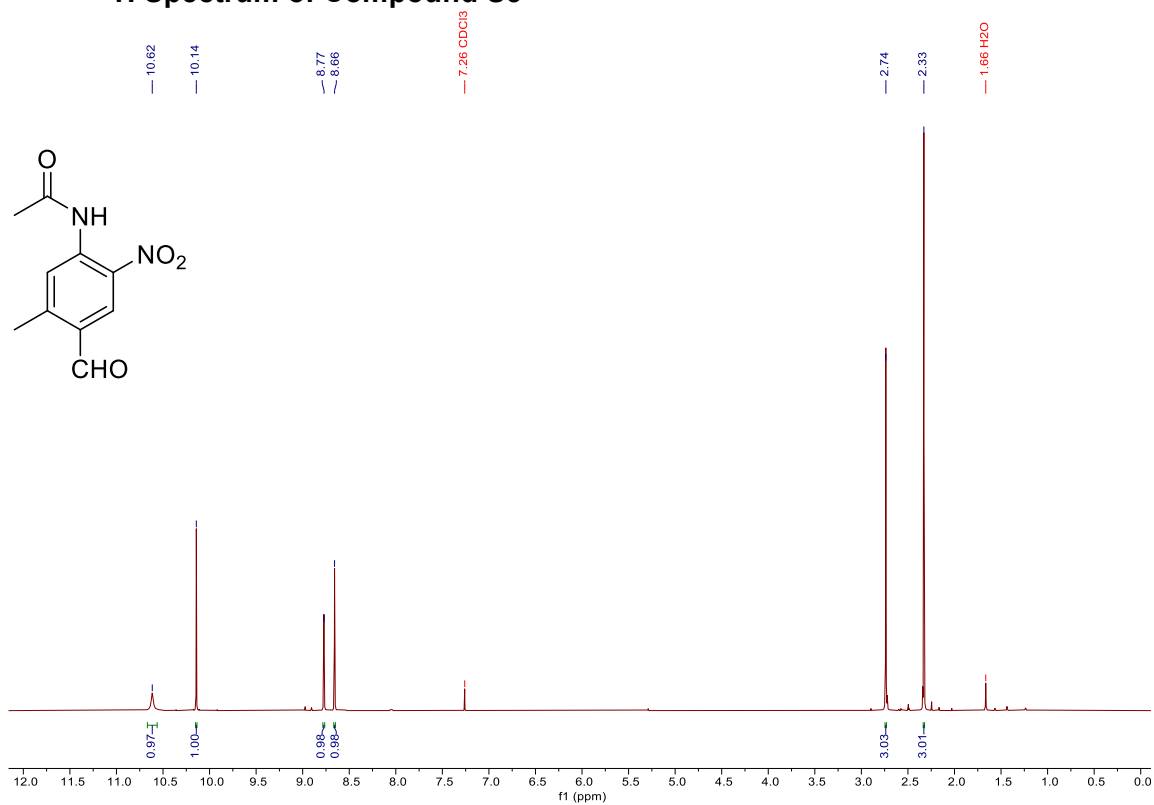
¹H Spectrum of Sensor 1a



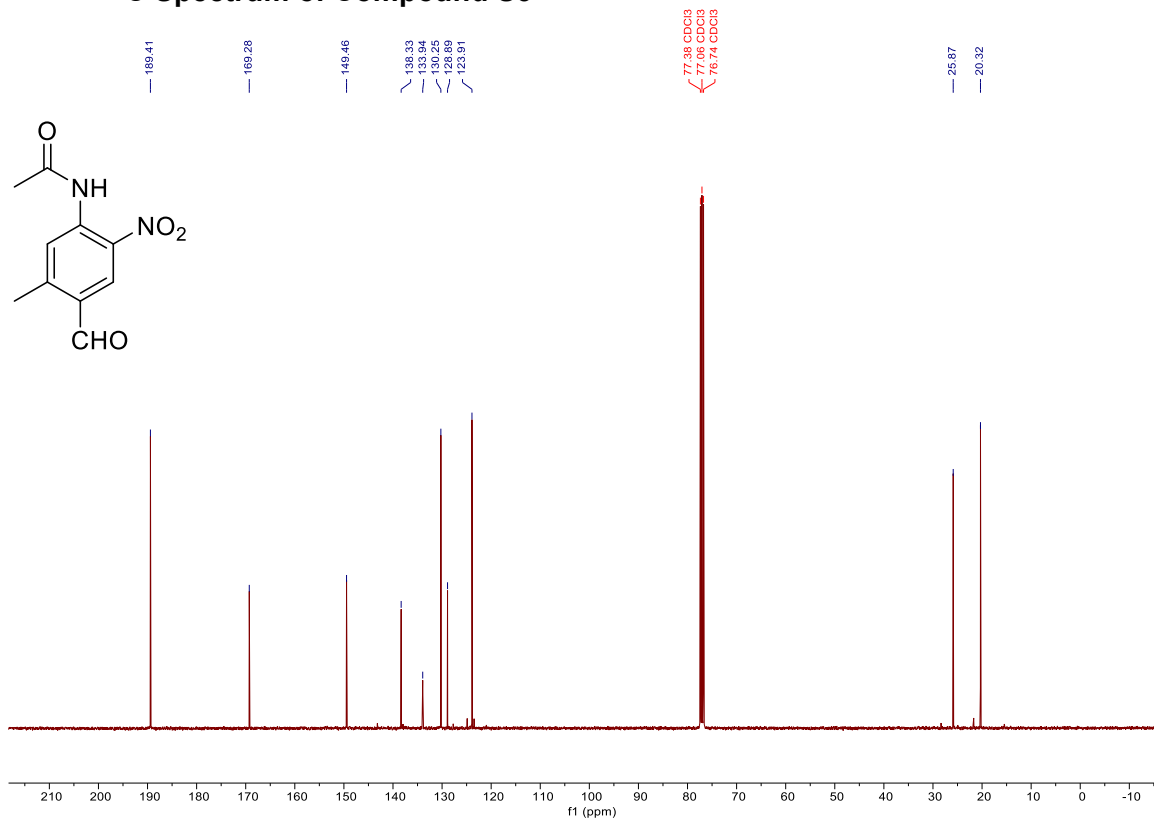
¹³C Spectrum of Sensor 1a



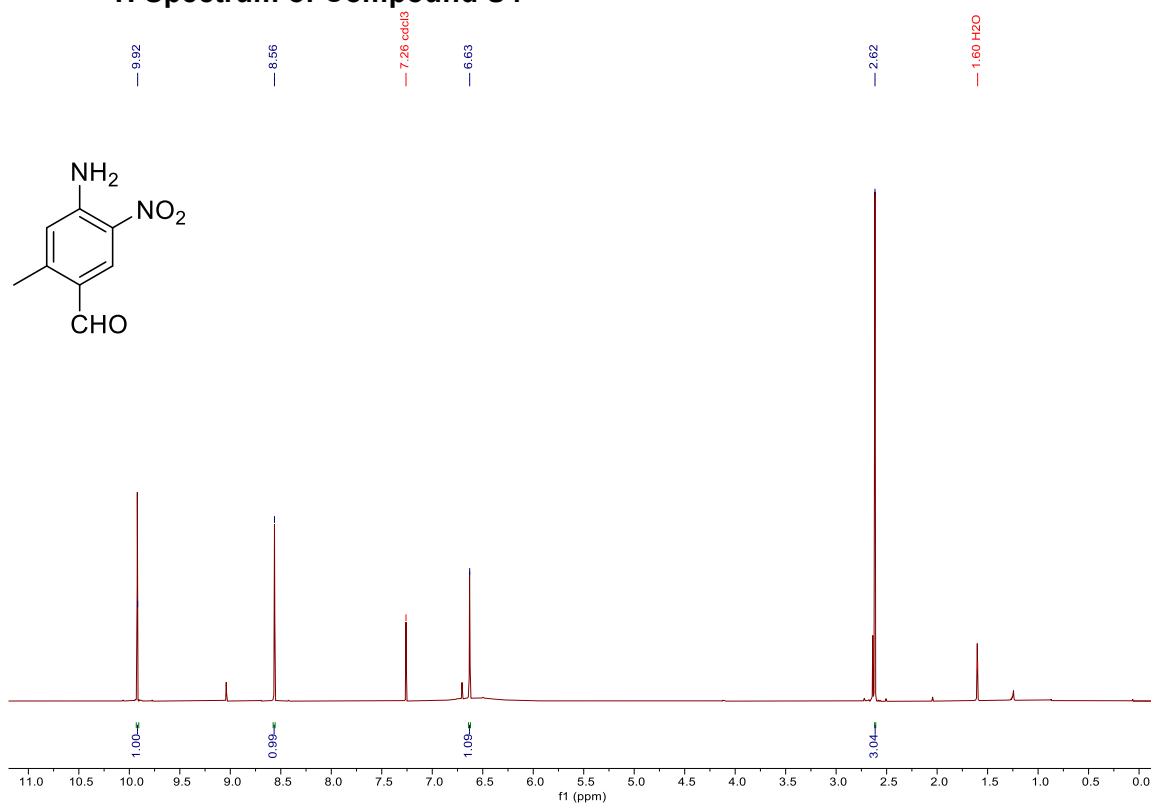
¹H Spectrum of Compound S3



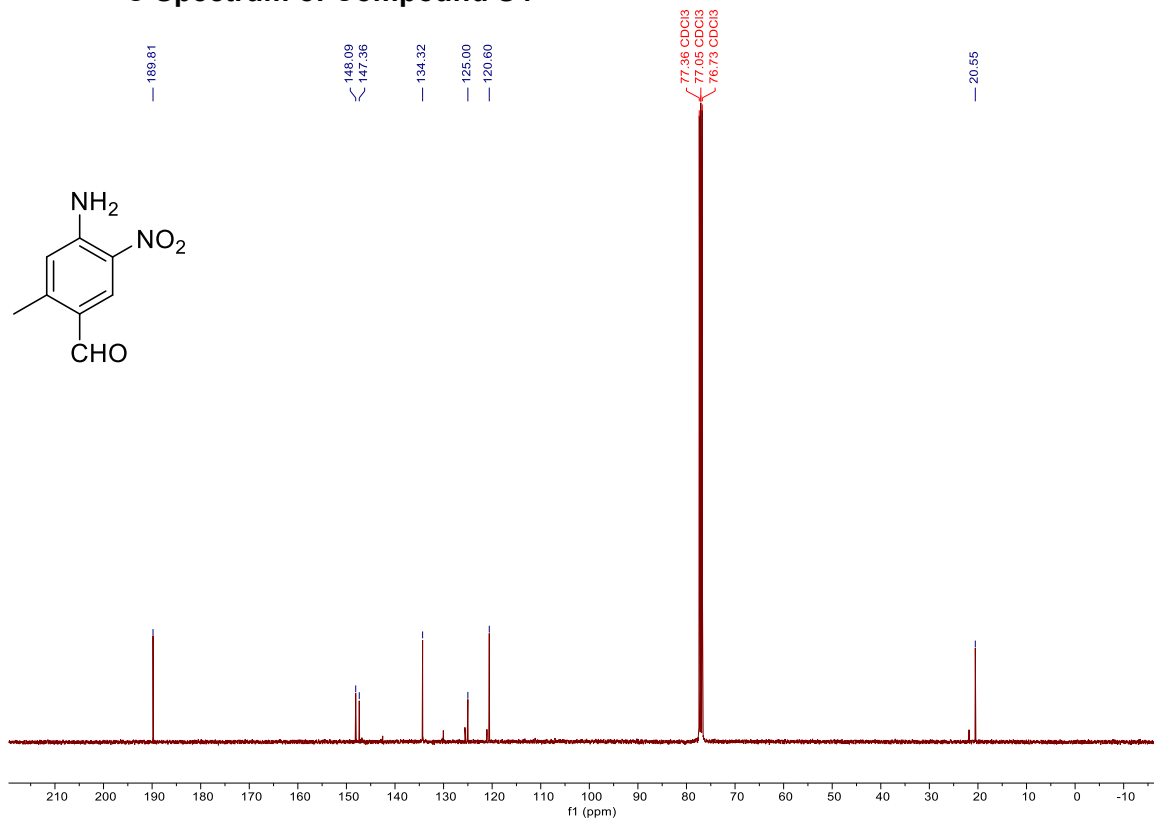
¹³C Spectrum of Compound S3



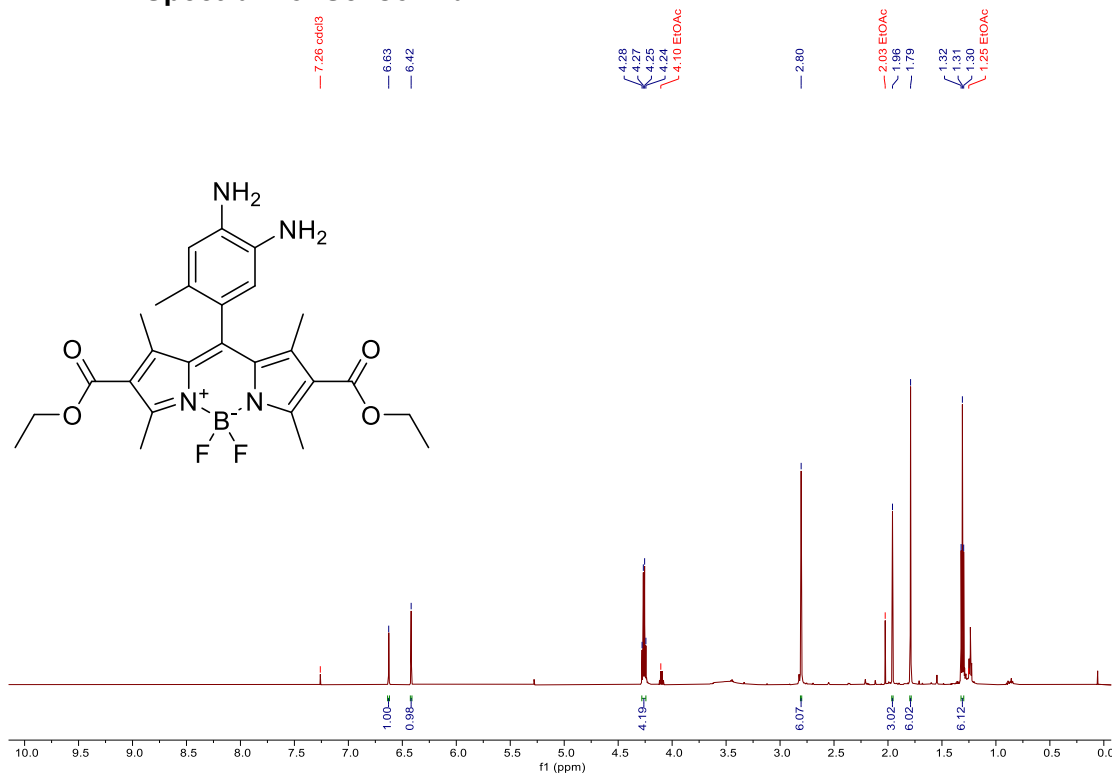
¹H Spectrum of Compound S4



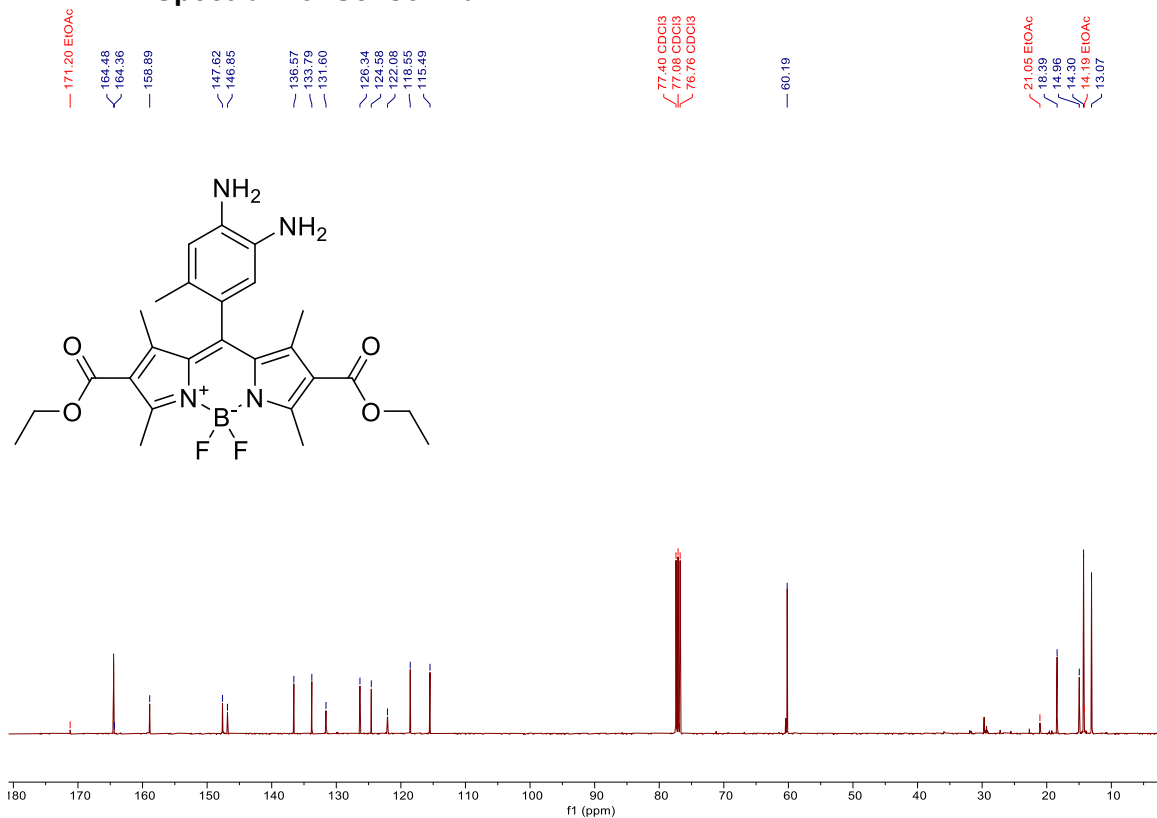
¹³C Spectrum of Compound S4



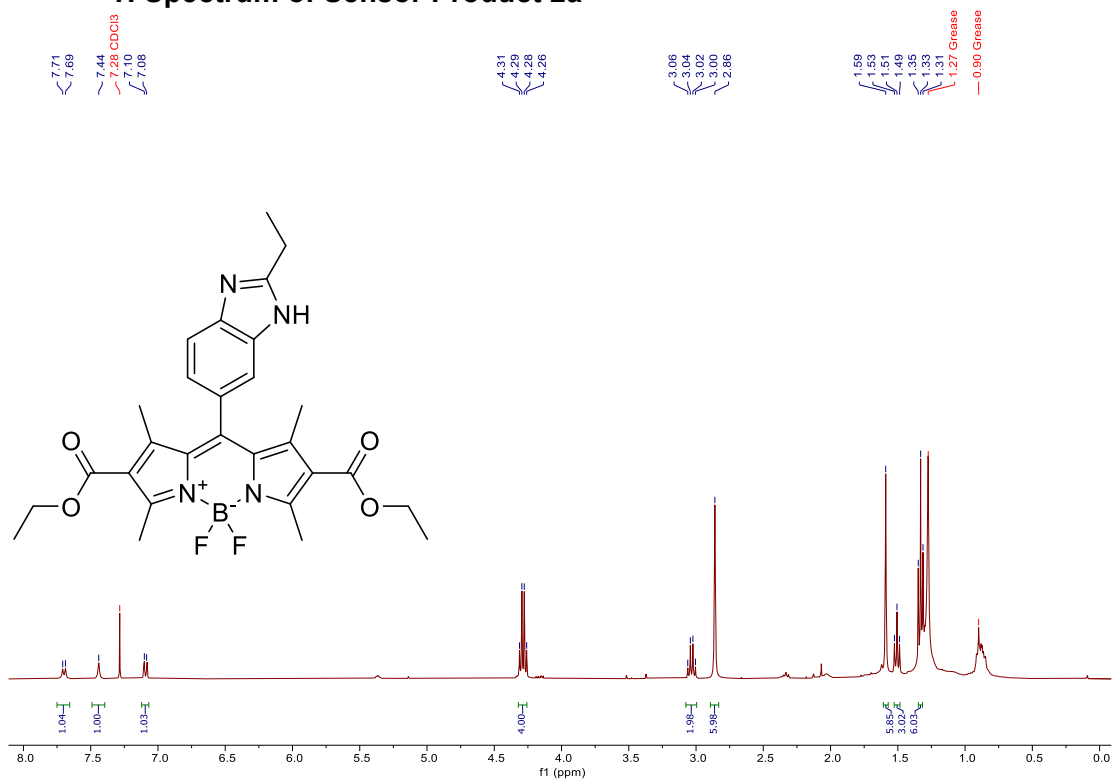
¹H Spectrum of Sensor 1b



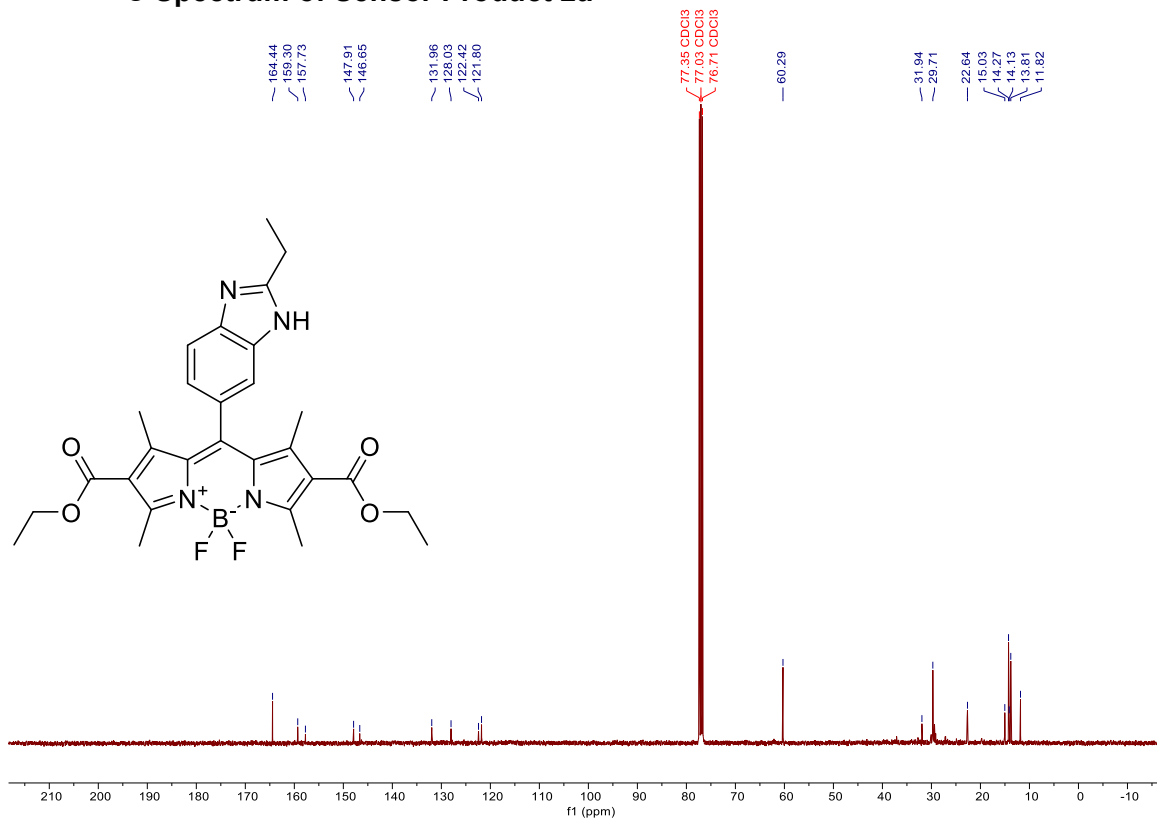
¹³C Spectrum of Sensor 1b



¹H Spectrum of Sensor Product 2a

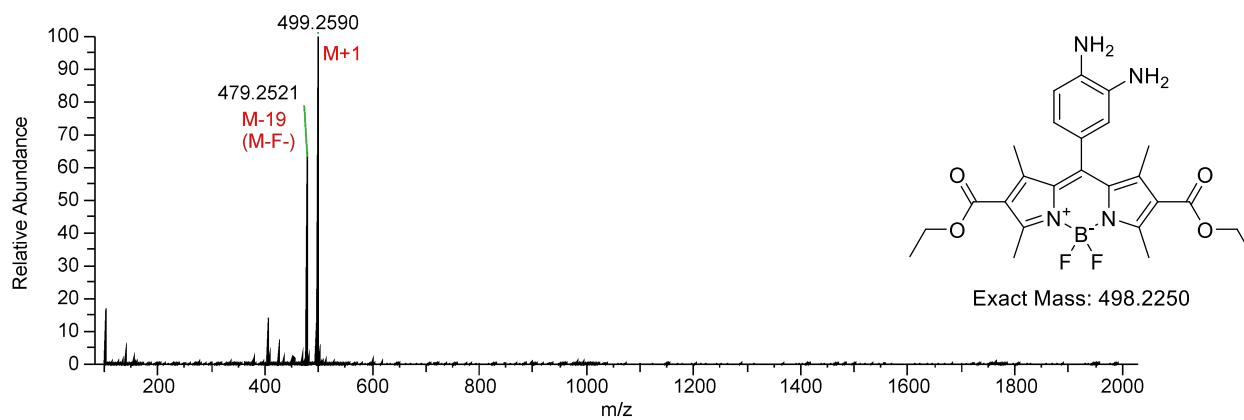


¹³C Spectrum of Sensor Product 2a

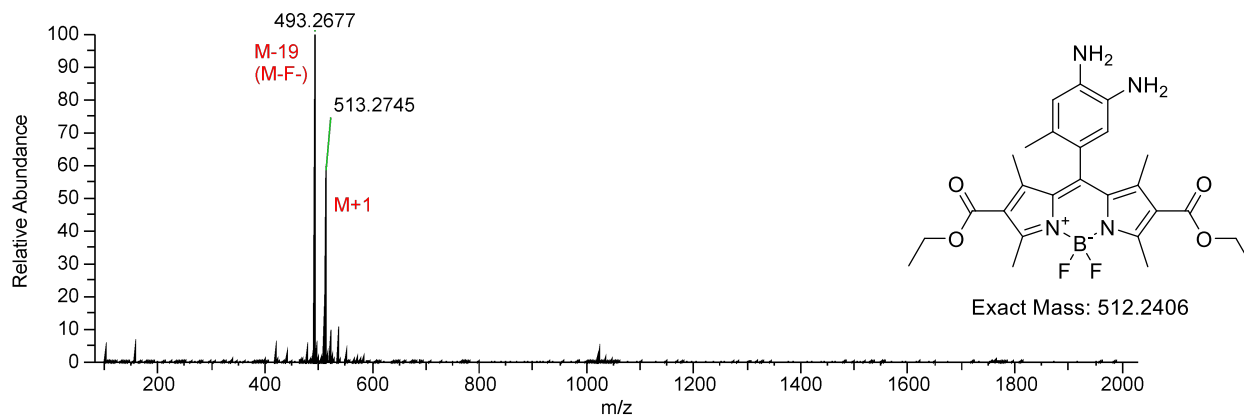


XXI. Supplementary Figure 15: HRMS spectra of sensors and products

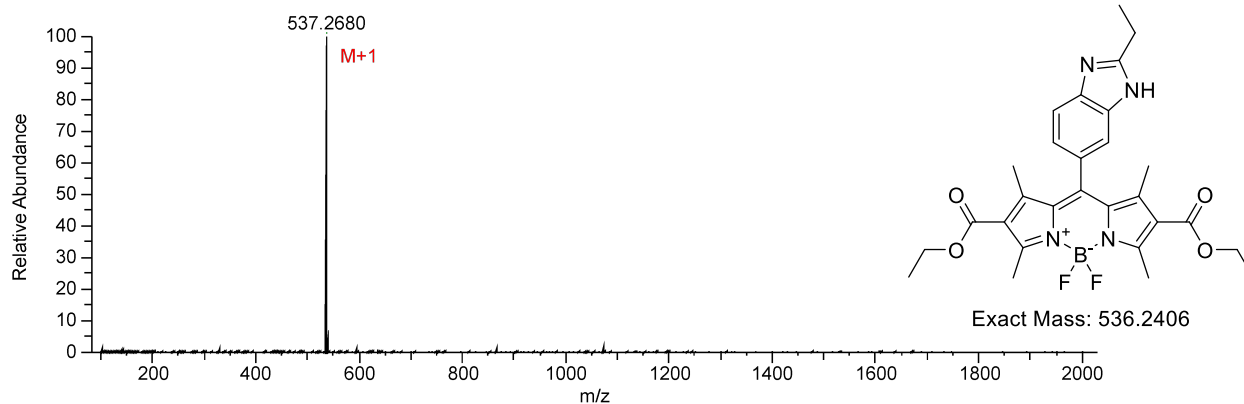
HRMS Spectrum of Sensor 1a



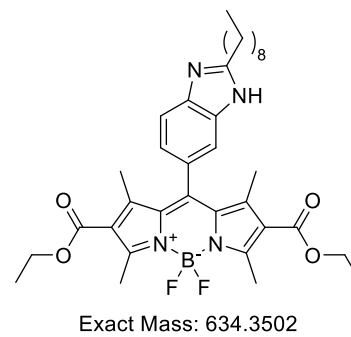
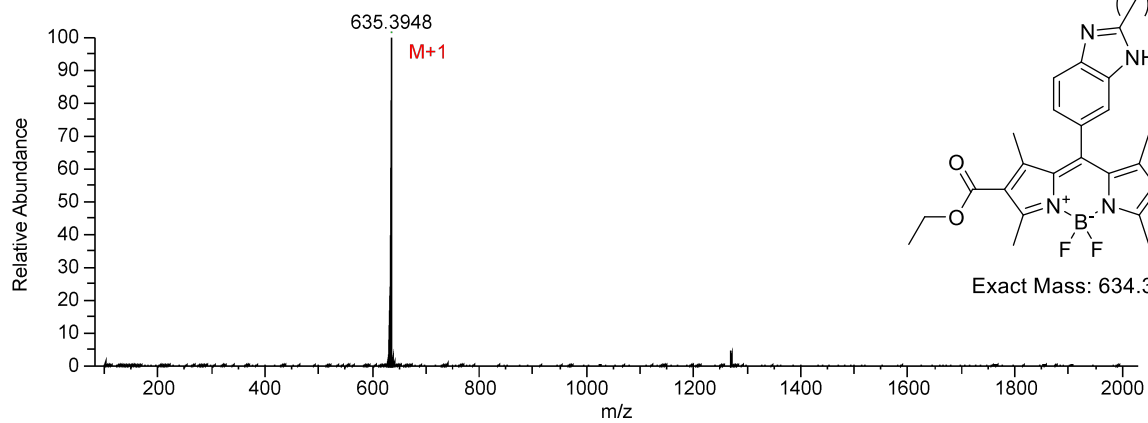
HRMS Spectrum of Sensor 1b



HRMS Spectrum of Sensor Product 2a



HRMS Spectrum of Sensor Product 3a



XXII. References

1. Wang, T.; Douglass, E. F.; Fitzgerald, K. J.; Spiegel, D. A. A “turn-on” fluorescent sensor for methylglyoxal. *J. Am. Chem. Soc.* **135**, 12429 (2013).